LOW TEMPERATURE NITROGEN BAKING OF A SRF CAVITY*

P. N. Koufalis†, F. Furuta, M. Ge, D. Gonnella[1], J. J. Kaufman, M. Liepe, J. T. Maniscalco, R. D. Porter
Cornell University, CLASSE, Ithaca, NY, USA
[1] also at SLAC National Accelerator Laboratory, Menlo Park, CA, USA

Abstract

We present the effects of a low temperature 160 °C nitrogen bake on the performance of a single-cell 1.3 GHz niobium cavity. The cavity demonstrated the same increase in quality factor, Q_0, and anti-Q-slope typical of cavities nitrogen-doped at 800°C reaching a maximum Q_0 of 3.6×10^{10} at E_{acc} = 16 MV/m and T = 2.0 K. Compared to the doping procedures in the high temperature regime, this method requires no post-treatment chemical etching.

INTRODUCTION

Impurity doping has been a topic of recent interest in the superconducting radio frequency (SRF) community, with much of the current focus on nitrogen as an interstitial impurity in bulk-niobium cavities. Previous experiments [1–3] have shown that nitrogen doping has the potential to increase cavity quality factor, Q_0, by a factor of two or more and gives rise to the so-called "anti-Q-slope". Until very recently, nitrogen doping has typically been done in the temperature regime ($T \geq 800$ °C) where niobium nitrides form on the surface, necessitating post-treatment chemical etching. Our focus here is on the nitrogen bake of a SRF cavity in the low temperature regime ($T \leq 200$°C) based on previous work at Fermilab [4] where nitride formation is not an issue and post-treatment chemistry is not needed. We show that low temperature nitrogen baking leads to cavity performance on par with cavities prepared in the high temperature regime.

CAVITY PREPARATION

A single-cell ILC-shaped 1.3 GHz bulk-niobium cavity, LTE1-4, received a chemical etching to ensure the removal of any contaminants or prior dopants, followed by a low temperature nitrogen bake at 160 °C and subsequently a long annealing period. The preparation procedure is outlined below:

1. Outside buffer chemical polish (10 min)
2. Inside vertical electropolish (16 µm)
3. 800 °C (12 hr in UHV)
4. 160 °C (48 hr in 35 mTorr N_2)
5. 160 °C (168 hr in UHV)

The degassing step (i.e. T = 800°C) removes hydrogen introduced by the BCP and EP and diffuses the oxygen from the oxide layer deep into the bulk. The nitrogen baking step exposes the the cavity surface to nitrogen gas and the annealing step allows for any nitrogen taken up by the surface diffuse further into the bulk

RF TESTING

Following the low temperature nitrogen bake, the cavity was rinsed on a high-pressure rinsing system before being assembled and tested. Measurements of cavity Q_0 vs. E_{acc} were taken at T = 2.0 K and are shown in Fig. 1. Anti-Q-slope and improvement in Q_0 are evident. The Q_0 continued to rise to a maximum of $3.6{\times}10^{10}$ at E_{acc} = 16 MV/m before gradually decreasing.

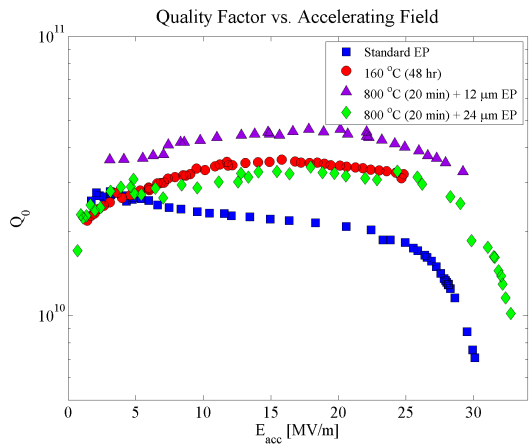

Figure 1: Cavity Q_0 vs. E_{acc} at T = 2.0 K. Both the high and low temperature treatments in a nitrogen atmosphere produce an anti-Q-slope and increased Q_0 compared to the baseline test (squares) of a standard niobium cavity.

For comparison, Q_0 vs. E_{acc} data taken previously from two high temperature (800 °C) doped cavities are shown in Fig. 1. A standard bulk niobium cavity is shown as well to serve as a performance baseline. The two doped cavities were treated in a nitrogen atmosphere at 800 °C for 20 min followed by a 30 min anneal at the same temperature in ultra-high vacuum. Each had a different amount of post-treatment material removal via vertical electropolishing. The cavity with the low temperature nitrogen treatment performs similarly to the doped cavity with the 24 µm EP removal in the medium field region but does not quite reach the same level of performance as the cavity with the 12 µm of material removal. Both quantitatively and qualitatively, the low temperature treatment and high temperature doping produce very similar results.

Figure 3 shows the deconvolution of R_{BCS} and R_0 at 2.0 K where these are the temperature dependent and independent

* Work supported by NSF Award PHYS-1416318
† pnk9@cornell.edu

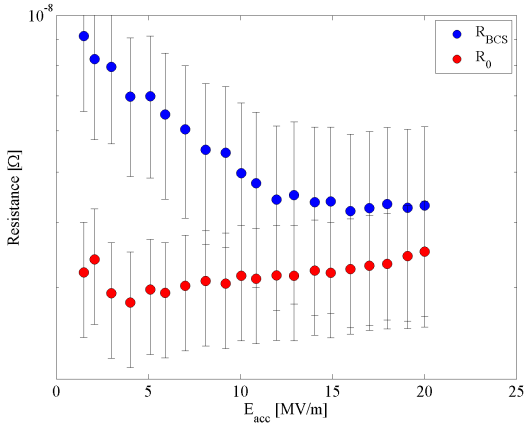

Figure 2: Deconolution of the temperature dependent, R_{BCS}, and independent, R_0, components of the surface resistance at 2.0 K as a function of accelerating field, E_{acc}.

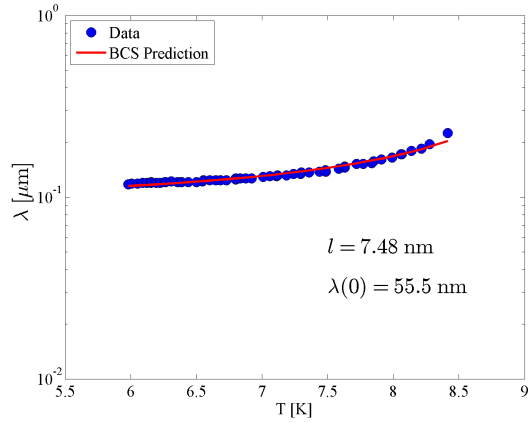

Figure 3: Fit of penetration depth vs. temperature with the fit parameters $\lambda(0)$ and l.

components of the surface resistance, respectively. The residual resistance, R_0, has little dependence on E_{acc} whereas R_{BCS} depends strongly on E_{acc}. This demonstrates that R_{BCS} is the component primarily responsible for the anti-Q-slope.

BCS FITTING

Material parameters were extracted using the code called SRIMP developed by J. Halbritter and based on the Matthis-Bardeen theory [5]. To extract the penetration depth, $\lambda(T = 0)$, and electronic mean free path, l, measurements of resonant frequency, f, as a function of T must be taken near T_c. The resonant frequency is first used to calculate the penetration depth $\lambda(T)$ vs. T using

$$\lambda(T) = \lambda(T_0) - \frac{1}{\beta}\left(f(T) - f(T_0)\right) \qquad (1)$$

where β =24 kHz/μm and T_0 is a reference point typically chosen between 6.5 and 8.5 K [6]. The $\lambda(T)$ vs. T data is then fit using SRIMP with $\lambda(T = 0)$ and l as fit parameters. Figure 3 shows the fit of the penetration depth and the corresponding extracted material parameters.

From measurements of Q_0 vs. T at low fields the surface resistance, R_S, is calculated using the fact that R_S is related to Q_0 by [7]:

$$R_S = G/Q_0 \qquad (2)$$

where $G = 278\ \Omega$ is the geometry factor of the cavity. Then SRIMP fits R_S vs. T with the normalized energy gap, $\Delta(0)/k_BT_c$, and the residual resistance, R_0, as free parameters. The results of this fit are shown in Fig. 4.

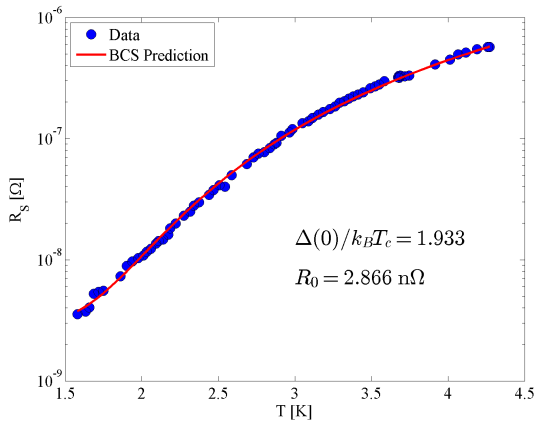

Figure 4: Fit of the surface resistance vs. temperature with the extracted material properties $\Delta(0)/k_BT_c$ and R_0.

DATA ANALYSIS

From the SRIMP fits of the low temperature treatment cavity, the residual resistance $R_0 = 3$ nΩ. This is consistent with the Q_0 vs. E_{acc} observed in Fig. 1 and typical values of residual resistance found in nitrogen doped cavities [2]. The energy gap does not deviate significantly from that of a standard niobium cavity or from a high-temperature nitrogen-doped cavity [2].

The mean free path $l = 7.5$ nm is relatively short compared to most typical doped cavities [2] and corresponds to a heavy doping. The temperature dependent component of the surface resistance R_{BCS} has a minimum at an optimal mean free path occurring at approximately 20 nm. The cavity in Fig. 1 with the 12 μm EP has a mean free path $l = 34 \pm 10$ nm whereas the cavity with a 24 μm EP has $l = 47 \pm 14$ nm. Being on either side of the minimum, LTE1-4 and the 24 μm EP cavity have a higher overall R_{BCS} leading to the slight degradation in performance.

Considering both the mean free path and relative performance of LTE1-4, it appears that nitrogen has diffused at least into the RF penetration layer $\lambda(0) \approx 60$ nm to affect performance in a way similar to high temperature doping. However, it is not certain whether this is definitely the case. Sample analysis would need to be completed to find the nitrogen concentration as a function of depth into the bulk to compare it to the doped cavities. Considering the very short mean free path, it should have a relatively high concentration

ISBN 978-3-95450-169-4

of nitrogen in the penetration layer. If it is found that the concentration of nitrogen is in fact not appreciable, it could be a high concentration of vacancies or other impurities that are causing the increased performance.

CONCLUSION

The advantage of low temperature nitrogen treatments is the increased performance without the chemical etching required of the cavities doped at higher temperatures. From the initial test, it is evident that there are little to no lossy nitrides present in LTE1-4. However, further tests need to completed to determine whether it is in fact nitrogen diffusing into the niobium in the low temperature treatment. It is possible that vacancies or other impurities are causing the change in behavior. In the future, we plan to do x-ray photoelectron spectroscopy (XPS) to determine the nitrogen concentration in the first 10 to 20 nm of the surface. Furthermore, cavities baked at various temperatures will also be tested to obtain a distribution of mean free paths and cavity RF performance data.If it is indeed nitrogen, it would be prudent to obtain measurements of the sensitivity to trapped magnetic flux as it has been shown that nitrogen doped cavities are more sensitive to trapped flux leading to high residual resistances.

REFERENCES

[1] A. Grassellino *et al.*, "Nitrogen and Argon Doping of Niobium for Superconducting Radio Frequency Cavities: A Pathway to Highly Efficient Accelerating Structures," *Supercond. Sci. Tech.*, vol. 26, no. 102001, Aug. 2013.

[2] D. Gonnella, "The Fundamental Science of Nitrogen-doping of Niobium Superconducting Cavities," Ph.D. thesis, Dept. of Physics, Cornell University, Ithaca, NY, USA, 2016.

[3] A. D. Palczewski, R. L. Geng, and C. E. Reece, "Analysis of High-Q_0 SRF Cavity Tests by Nitrogen Gas Doping at Jefferson Lab," in *Proc. 27th Lin. Accel. Conf. (LINAC14)*, Geneva, Switzerland, Sep. 2014, paper TUPP138, pp. 736–739.

[4] A. Grassellino and S. Aderhold, "New Low T Nitrogen Treatment Cavity Results with Record Gradients and Q," *TESLA Technology Collaboration*, Saclay, France, July 2016.

[5] J. Halbritter, "FORTRAN Program for the Computation of the Surface Impedance of Superconductors," KAROLA Externer Bericht, 3/70-6, 1970.

[6] G. Ciovati, "Effect of Low-temperature Baking on the Radio-frequency Properties of Niobium Superconducting Cavities for Particle Accelerators," *J. Appl. Phys.*, vol. 96, no. 3, Aug. 2004.

[7] H. Padamsee, J. Knobloch, and T. Hays, *RF Superconductivity for Accelerators*, New York, NY, USA: Wiley, 1998.